Sensors and Actuators A 189 (2013) 399–408

Contents lists available at SciVerse ScienceDirect

Sensors and Actuators A: Physical

journal homepage: www.elsevier.com/locate/sna

Synthesis and characterization of Cu-doped ZnO one-dimensional structures for miniaturized sensor applications with faster response

L. Chow[a,b,*], O. Lupan[a,c,*], G. Chai[a], H. Khallaf[a], L.K. Ono[a], B. Roldan Cuenya[a,d,e], I.M. Tiginyanu[f,g], V.V. Ursaki[f,g], V. Sontea[c], A. Schulte[a]

[a] Department of Physics, University of Central Florida, PO Box 162385, Orlando, FL 32816-2385, USA
[b] Graduate Institute of Electro-Optical Engineering and Green Technology Research Center, Chang Gung University, Tao-Yuan, Taiwan, 333 Republic of China
[c] Department of Microelectronics and Semiconductor Devices, Technical University of Moldova, 168 Stefan cel Mare Blvd., MD-2004 Chisinau, Republic of Moldova
[d] Department of Civil, Environmental and Construction Engineering, University of Central Florida, USA
[e] Nanoscience Technology Center, University of Central Florida, Orlando, FL, USA
[f] Laboratory of Nanotechnology, Institute of Electronic Engineering and Nanotechnologies, Institute of Applied Physics of the Academy of Sciences of Moldova, MD-2028 Chisinau, Republic of Moldova
[g] National Center for Materials Study and Testing, Technical University of Moldova, MD-2004 Chisinau, Republic of Moldova

ARTICLE INFO

Article history:
Received 3 June 2012
Received in revised form 22 August 2012
Accepted 8 September 2012
Available online 29 September 2012

PACS:
81.05.Dz
81.07.Bc
81.16.Be
07.07.Df
81.16.–c
85.35.–p

Keywords:
ZnO
Crystal
Sensor
Microrod
Cu-doping

ABSTRACT

Detection of chemicals and biological species is an important issue to human health and safety. In this paper, we report the hydrothermal synthesis at 95 °C of Cu-doped ZnO low-dimensional rods for room-temperature (RT) sensing applications and enhanced sensor performances. X-ray diffraction, scanning electron microscopy, X-ray photoelectron spectroscopy, Raman and photoluminescence are used to characterize the material properties. To demonstrate the suitability of the Cu-doped ZnO rods for gas sensor applications and for comparison with pure ZnO, we fabricated a double rod device using Focused Ion Beam. The responses of pure-ZnO and Cu-doped ZnO rods studied in exactly the same condition are reported. We found that Cu-ZnO sensors have enhanced RT sensitivity, faster response time, and good selectivity. Miniaturized Cu-ZnO rod-based sensors can serve as a good candidate for effective H_2 detectors with low power consumption.

1. Introduction

Recently, increasing attention has been paid to the utilization of hydrogen as a renewable and clean energy source because it provides a timely solution to the future energy supply [1,2] in addition to other renewable energies. Thus, hydrogen gas detection measurements became an essential step for safety in industrial and household places to alert the formation of potentially explosive mixtures with air [3]. Another significant demand on rapid and accurate sensors able to monitor and control hydrogen concentration is in industrial processes where hydrogen is used in synthesis or chemical reactions, as well as for nuclear reactor safety [3]. A main issue in hydrogen sensor technology is the development of higher sensitivity, higher selectivity, and faster detection mechanisms. Although current hydrogen sensor technologies [4,5] are suitable for many industrial applications, some of them are not appropriate for fuel cells, household, biomedical, and transportation applications because of their size, high temperature operation, slow response, high cost, and energy input [6]. Individual one-dimensional metal oxide structures have become promising candidates for hydrogen sensing applications in recent years due to their special geometry and chemical–physical properties [7–11]. In such gas sensors the change in the electrical resistance

* Corresponding authors at: Department of Physics, University of Central Florida, PO Box 162385, Orlando, FL 32816-2385, USA. Tel.: +1 407 823 2333; fax: +1 407 823 5112.
E-mail addresses: Lee.Chow@ucf.edu (L. Chow), Lupanoleg@yahoo.com (O. Lupan).

0924-4247/$ – see front matter © 2012 Elsevier B.V. All rights reserved.
http://dx.doi.org/10.1016/j.sna.2012.09.006

is due to the interaction of the targeted gas molecules (chemi or physisorption) with the surface of the ZnO micro/nanorod [10,12]. However, in practice, such sensors are not competitive due to their slow response, sensitivity and selectivity issues [10,12]. In addition, such sensors need to be operated at high temperatures [11,13,14]. Working at high temperatures should be avoided because the H_2 may burn in air before reaching the surface of the sensing material at temperatures > 500 °C) [15]. Thus, for H_2 sensor applications zinc oxide micro/nanostructures have to demonstrate improved performances, integrated circuit compatibility, and ability to work at room temperature in H_2 sensor applications.

In this context, we studied surface functionalization and doping of ZnO rods/wires to improve their sensing properties [10,12,14] by modifying material properties. Doping nanocrystals is a major challenge in the future applications of nanomaterials [16]. The Cu doping of ZnO materials has been a very active research area in the last few years, mostly due to the interesting ferromagnetic properties of Cu-doped ZnO [17–24]. However, there have been only a few reports on the effects of Cu doping on the sensing properties of ZnO [25–29]. For example, Sonawane et al. [25] reported gas sensing properties of nanocrystalline ZnO:Cu for different concentrations of Cu and found for 1 wt% Cu in zinc oxide a higher response and selectivity to H_2. Paraguay et al. [26] used the spray pyrolysis technique to obtain ZnO films doped with Cu and investigated the ethanol sensing at temperatures ranging between 435 and 675 K. Gong et al. [27] used co-sputtering technique to obtain Cu-doped ZnO films for CO sensing at temperatures of 150–400 °C. More recently Zhao et al. [28] used electrospinning to fabricate Cu-doped ZnO nanofibers for H_2S sensing application. Ghosh et al. [29] investigated the effect of Cu doping on the liquid propane gas sensing properties of soft chemically grown nano-structured ZnO thin films.

Here we present our investigation of the fabrication of Cu-doped ZnO rod-structures via rapid hydrothermal synthesis [30,31]. It is known that group Ib metals are fast diffusers in compound semiconductors [32,33]. The diffusion of Cu into ZnO can cause the formation of various centres (Cu_{Zn}, Cu_i). It is possible that Cu atoms can replace either substitutional or interstitial Zn atoms in the ZnO lattice creating structural deformations [21,34,35]. Cu significantly affects the electrical, chemical, structural and optical properties of ZnO, and the study of the electronic state of Cu in ZnO has been the subject of interest for a long time [33,36–40]. Recently, Xing et al. [41] found a clear evidence of the ultrafast charge transport process between the ZnO host and the Cu dopants in Cu-doped ZnO nanowires (NWs) with a time constant of about 39 ± 9 ps. All these new properties of Cu-doped ZnO are very attractive for designing RT sensor with faster response to H_2 gas.

In this work, we report the properties of Cu-ZnO rod-structures and a comparison of pure and Cu-doped ZnO single rod hydrogen sensors with improved performances at room temperature. We discuss the procedure to improve the dynamics in H_2 sensing by an individual Cu-doped ZnO micro-rod gas sensor.

2. Experimental

ZnO and Cu-doped ZnO low-dimensional rods were grown by a procedure discussed in details in previous reports [31,42]. *p*-type Si(1 0 0) substrates were used for the synthesis of the ZnO and Cu-ZnO material. First, the silicon (Si) substrates were cleaned as reported before [43]. All the chemical reagents used in our experiments were of analytical grade and without further purification. Zinc sulfate heptahydrate [$Zn(SO_4)\cdot 7H_2O$] was first dissolved into 100 ml deionized (DI) water and then 50 ml of ammonia (29.3%, Fisher Scientific) was added and stirred for 10 min to mix completely at room temperature. The first set of pure ZnO nanorods (#1) samples was synthesized using 0.1–0.5 M of $Zn(SO_4)\cdot 7H_2O$ [42]. A second set of samples (#2) was prepared using 0.1–0.5 M of zinc sulfate and 0.001–0.005 M of copper chloride (99.99%) which was dissolved in 100 ml DI water. The [Cu]/([Zn]+[Cu]) ratio of copper dopants in the ZnO rods was controlled by changing the relative amount of Cu to Zn in the precursor solution. An ammonia solution (29.3%) was added until the solution became transparent and clear. Subsequently, the resulting aqueous solution was poured into a 120 ml reactor (75% filled) [42]. The vessels were placed on a preheated oven for 15 min and 20 min at 95 °C and then allowed to cool down to room temperature in 40 min. After the reaction was completed, the ZnO nanorods grown on the substrates were rinsed in deionized water for 2 min and then the samples were dried in air at 150 °C for 5 min. Manipulation and reactions were carried out in air inside a fume hood.

The size and morphology of the samples with ZnO nanorods were observed with a JEOL scanning electron microscope (SEM). The compositional analysis of the ZnO nanorods was carried out using Energy dispersive X-ray spectroscopy (EDX), in combination with SEM.

X-ray powder diffraction (Rigaku 'DB/MAX' powder diffractometer) was used for structural analysis for Bragg angles (2θ) ranging from 5° to 90° using Cu K_α radiation ($\lambda = 1.54178$ Å).

The ex situ prepared samples were mounted on a molybdenum sample holder and subsequently transferred into an ultrahigh vacuum (UHV) system equipped with a hemispherical electron energy analyzer (Phoibos 100, SPECS GmbH) and a dual-anode (Al K_α, 1486.6 eV and Ag L_α, 2984.4 eV) monochromatic X-ray source (XR50 M, SPECS GmbH). The base pressure in the analysis chamber during the XPS measurements was $\sim 6 \times 10^{-10}$ mbar. For the quantitative analysis of the peak positions and relative spectral areas of the Zn-2p, Cu-2p, O-1s and C-1s components, the raw XPS spectra were fitted with Gaussian–Lorentzian functions. Due to spin-orbit coupling, the intensity ratios between the $2p_{3/2}$ and $2p_{1/2}$ (Zn and Cu) doublets were held constant at a value of 2. The concentration of the Cu dopant relative to ZnO was estimated from the Cu-2p/Zn-2p ratio after proper normalization using the atomic sensitivity factors (ASF) recommended by the manufacturer of our XPS system.

The continuous wave (cw) photoluminescence (PL) was excited by the 325 nm line of a He–Cd Melles Griot laser. The emitted light was analyzed with a double spectrometer with a spectral resolution better than 0.5 meV. The signal was detected by a photomultiplier working in the photon counting mode. The samples were mounted on the cold station of a LTS-22-C-330 optical cryogenic system.

Information on vibrational modes in pure and doped ZnO nanorods was obtained from Raman backscattering experiments in a micro-Raman setup Horiba Jobin Yvon LabRam IR spectrometer with a charge-coupled detector (CCD). This system has a spatial resolution of 2 μm. Raman spectra were excited with 1.96 eV photons from a Helium Neon laser ($\lambda \sim 633$ nm) with less than 4 mW of power at the sample. The spectral resolution was better than 2 cm^{-1}, and the instrument was calibrated using a naphthalene standard.

The gas response was measured using a two-terminal ZnO rod device [8–10]. Its characteristics were measured using a semiconductor parameter analyzer with input impedance of 2.00×10^8 Ω. The fabricated device structure was put in an environmental chamber to detect different gasses (H_2, O_2, C_2H_5OH, CH_4 and natural gas-LPG). The humidity of the gas mixture was about 60 RH%. The gas flow was controlled by a mass flow controller (MKS) and test system as reported before [10,14].

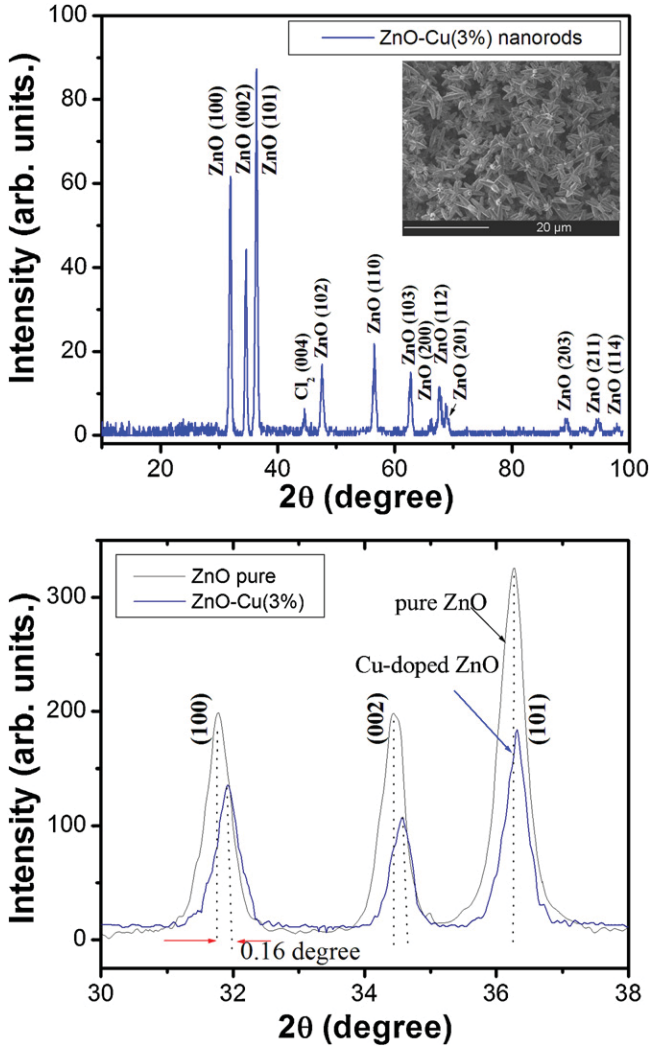

Fig. 1. (a) XRD patterns of the 3% Cu-doped ZnO nanorods on substrates. Insert shows an SEM image of 3% Cu-doped ZnO rods on SiO_2/Si(0 0 1). (b) Comparison of the (1 0 0), (0 0 2) and (1 0 1) peaks taken for pure ZnO and 3% Cu-doped ZnO.

3. Results and discussion

3.1. Structural analysis

A systematic investigation of Cu-doping effects on the properties of one dimensional ZnO structures was performed by using several techniques. The insert in Fig. 1 shows an SEM image of Cu-doped ZnO grown by a hydrothermal technique at 95 °C in 20 min. Low-dimensional rods of ZnO can be seen grown in agglomerations on the substrate. Later these structures can be transferred and dispersed on other substrates as described in previous work [8,31,42]. No differences in morphology were observed at concentration as low as 0.5% Cu in comparison with pure ZnO reported previously [8,9]. Fig. 1 shows the XRD patterns of the Cu doped ZnO nanorods deposited at 95 °C. The intense diffraction peaks of the ZnO deposition appear at 31.77, 34.43, 36.27, 47.53, 56.61 and 62.83, which correspond to the (1 0 0), (0 0 2), (1 0 1), (1 0 2), (1 1 0) and (1 0 3) planes, respectively. The intense peaks in the XRD pattern of these samples clearly show the formation of the hexagonal wurtzite structure of ZnO (space group: $P6_3mc$(186) or C_{6v}^4 (Schoenflies notation); a = 0.3249 nm, c = 0.5206 nm). The prominent (0 0 2) plane is observed in all samples (0–3% Cu in ZnO), which is the most dense plane in wurtzite ZnO [44].

It was also observed that with increasing Cu concentration (from 0 to 3 at%) the intensity of the ZnO peaks decreased (not shown) which was caused by the decreases in the crystallinity of ZnO. The (0 0 2) peak positions 2θ of the doped sample were shifted to a higher value for the higher dopant concentrations 34.44 and 34.60, respectively. The shift in the (0 0 2) peak for Cu-doped ZnO might be due to the substitution of Zn by Cu in the hexagonal lattice. These shifts agree with previous reports [45–47]. Such changes in crystallinity might be the result of changes in the atomic environment due to extrinsic doping of ZnO samples [45–47]. Note that differences in ionic radii ref. [48] should be considered. According to [48] the 4-fold coordinated Zn^{2+} and Cu^{2+} cations have ionic radii of 0.074 and 0.057 nm respectively, and stable electronic configurations: $Zn^{2+}(3d^{10})$ and $Cu^{2+}(3d^9)$. The 4-fold coordinated, Cu^{1+} has ionic radius of 0.06 nm $Cu^1(3d^{10})$ [48]. From XRD results, a slight lattice deformation was observed for Cu-doped ZnO and it could be due to the shorter Cu_{Zn}—O bonds, and smaller [Cu_{Zn}—O_4] units in Cu-doped ZnO rods [49]. No change in the crystalline structure was detected, which suggests that the majority of the Cu atoms were in the ZnO wurtzite lattice. It is known that similarly to most group II–VI materials, the bonding in ZnO is largely ionic (Zn^{2+}–O^{2-}), which favors doping with Cu. According to theoretical calculations by Yan et al. [50] on Cu-ZnO electronic structure, Cu occupying a Zn site creates a single-acceptor state above the valence band E_v of ZnO. Due to the low formation energy of the Cu in ZnO under O-rich conditions, high concentration of dopants can be achieved with Cu [50]. According to our experimental XRD data, only ZnO peaks at concentrations of 0-3% Cu have been detected, which suggest its incorporation in the lattice. Lattice parameters of pure ZnO NWs, are a = 3.2505 Å, c = 5.2056 Å and for Cu-doped ZnO, a decrease was observed (3.2461 Å and 5.1977 Å, a and c respectively). The Cu-doping mechanism of ZnO NWs can be described by Cu-doping into the ZnO host lattice; Cu^{2+} and Cu^+ ions are substituting the Zn^{2+} sites as was analyzed in previous works [51,52]. The slight difference in lattice parameters of Cu-doped ZnO depositions is probably caused by the copper atoms occupying different positions in the ZnO lattice and by the formation of complex defects [Cu_{Zn}—Zn_i]^x in Cu-ZnO [33]. XRD data clearly show the effect of Cu doping in the ZnO lattice and that it does not contribute to phase segregation, which is an important issue for further sensor applications.

3.2. Chemical analysis

For a deeper understanding of chemical composition and bonding in Cu-doped ZnO structures, XPS analysis was employed. Fig. 2 shows an XPS survey spectrum of a Cu-doped ZnO sample supported on SiO_2/Si(0 0 1). The following elements were detected: Zn, O, Cl, N, and C. The BE scale was calibrated using the adventitious carbon peak (C-1s) at 285 eV [29]. Residual amounts of adventitious carbon and carbonyl compounds are unavoidable due to air exposure prior to the XPS measurements. In addition to the adventitious carbon peak, the C-1s XPS spectrum of our samples (not shown) also displays two additional peaks at 286.6 eV and 288.7 eV corresponding to C═O and O═C—O, respectively [31]. As will be described below, those peaks were used as reference in the determination of the different O species present in our samples.

Fig. 3 shows XPS spectra of the (a) Zn-2p, (b) Cu-2p, and (c) O-1s core level regions of the Cu-doped ZnO rods. A doublet at 1021.8 eV and 1044.9 eV is observed in (a) corresponding to the Zn-$2p_{3/2}$ and $2p_{1/2}$ core levels. These values are shifted to higher binding energies (BEs) by +0.4 eV when compared to similarly prepared pure ZnO rods previously measured by our group [31]. Similar positive BE shifts (+0.4 to +0.7 eV) were also observed for Sb- and Ag-doped ZnO rods [31]. The peak width (FWHM) of the Cu-doped ZnO rods was also found to be larger as compared to pure ZnO rods (2.2 eV versus 1.6 eV, respectively). Since the size of the ZnO rods

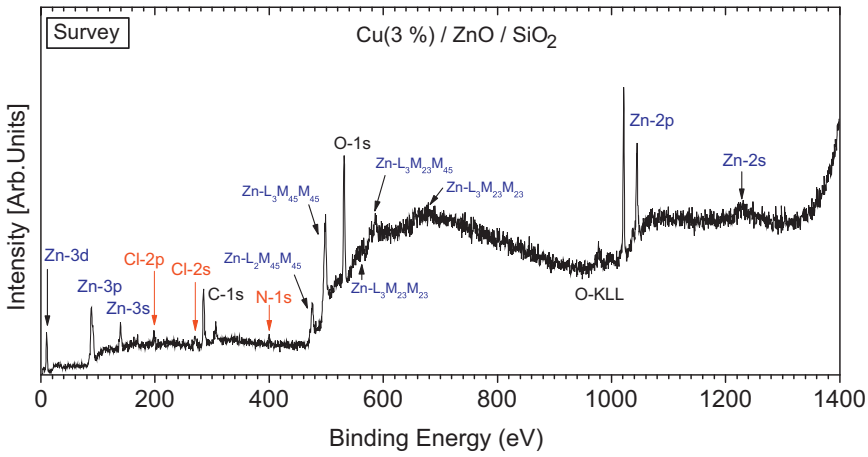

Fig. 2. Survey XPS spectra (Al K_α = 1486.6 eV) corresponding to Cu-doped ZnO rods supported on SiO_2/Si(0 0 1). In addition to Zn, other elements detected were O and adventitious C, Cl and N residues from the sample preparation method. The different photoelectron and Auger electron peaks observed for the latter elements are labeled in the graph.

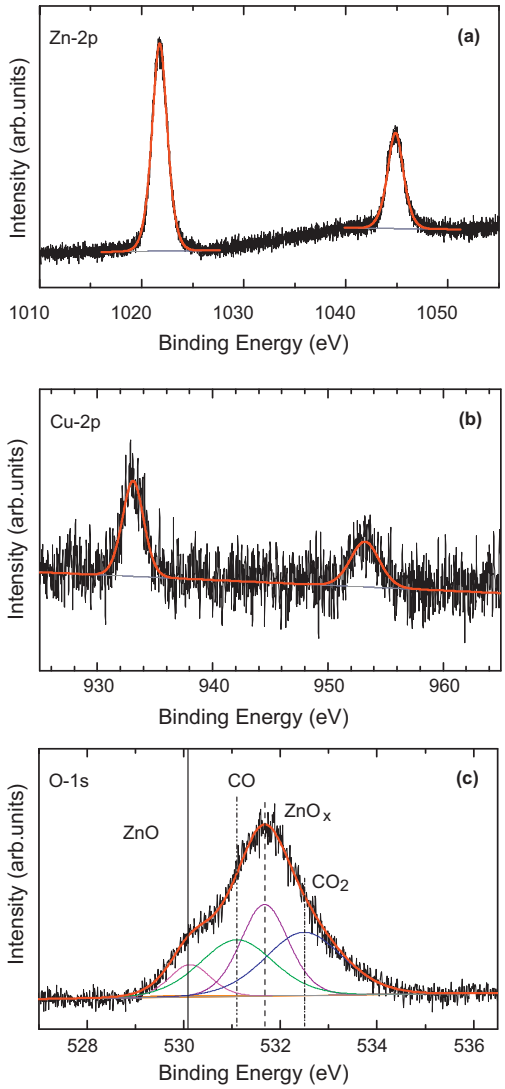

Fig. 3. XPS spectra (Al K_α = 1486.6 eV) corresponding to the (a) Zn-2p, (b) Cu-2p, and (c) O-1s core level of Cu-doped ZnO rods supported on SiO_2/Si(0 0 1).

is similar in both samples, the broadening of the Zn-2p XPS peaks suggests the presence of additional Zn states and/or defects within the ZnO structure [53–55]. No differences in XPS were observed for lower concentrations of Cu (0.5%) in comparison with pure ZnO [31].

The Cu-2p XPS binding energy region is shown in Fig. 3b. Photoelectron peaks corresponding to the Cu $2p_{3/2}$ and $2p_{1/2}$ core levels were observed at 933.1 eV and 953.5 eV. Literature references [31,56] report the following ranges for the BEs of Cu-$2p_{3/2}$ in metallic and cationic Cu species: 932.6 ± 0.2 eV for Cu^0, 932.5 ± 0.3 eV for Cu^+, and 933.6 ± 0.3 eV for Cu^{2+}. Nevertheless, it should be noted that the majority of those references correspond to bulk-like Cu samples, contrary to the case of our Cu-dopants. Although small differences were reported in the literature for metallic Cu and CuO, according to the measured BEs, the Cu species detected in our samples appear to be cationic (CuO or Cu—O—Zn compounds) [53,56]. We do not observe satellite peaks typical of CuO_2 (normally at ~942 eV and ~963 eV), therefore, we conclude that the most likely oxidation state of our dopant is Cu^+ [57,58]. Since some changes in the BE and width of the Zn peaks of ZnO were observed for the Cu-doped samples as compared to pure ZnO rods, the incorporation of Cu^+ ions into the ZnO lattice sites [59,60] (Cu—O—Zn) is inferred. An estimation of ~3 at.% Cu-doping in this sample was obtained based on the XPS integrated areas and the Cu-2p/Zn-2p ratio after proper normalization by the corresponding atomic sensitivity factor (ASF).

The asymmetric features observed in the O-1s region, Fig. 3c, were deconvoluted by several subspectral components: (i) O in ZnO (530.1 eV), (ii) O in defective ZnO_x, ZnOH and/or Cu—O—Zn (531.7 eV), (iii) adventitious CO (531.1 eV), and (iv) adventitious CO_2 (532.5 eV) [31]. In our previous investigations of undoped ZnO rods [31], the two main peaks observed at 530.2 eV and 531.6 eV were assigned to O^{2-} ions in stoichiometric Zn—O—Zn and non-stoichiometric $ZnO_x(OH)_y$, respectively. Interestingly, we have observed a significant increase in the ratio of the oxygen XPS feature attributed to defective ZnO in the Cu-doped sample (ZnO_x/ZnO = 3.3) as compared to the undoped ZnO (ZnO_x/ZnO = 0.5) [31] reemphasizing the incorporation of Cu^+ ions into the ZnO network [55,61–63] and the consequent generation of defects [31]. Thus, ternary compounds with Cu^+ ions occupying interstitial and/or substitutional sites (Cu_{Zn}) in ZnO are likely to be present in our sample [61–63]. The latter is in agreement with low energy ion scattering (LEIS) results by Jansen et al. [63] indicating the possibility of monovalent copper in Cu_{Zn}—V_O complexes (V_O represents oxygen vacancies). X-ray absorption spectroscopy data of Ma et al.

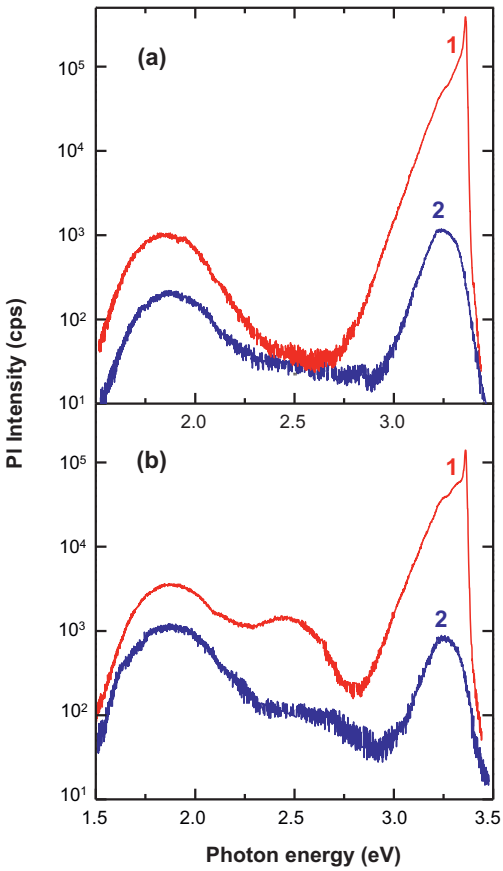

Fig. 4. PL spectra of: (a) 0.5% Cu-ZnO and (b) 3.0% Cu-ZnO rods measured at $T = 10$ K (curve 1) and $T = 300$ K (curve 2).

[49] from Cu-doped ZnO films suggested a $Cu_{Zn}O_4$ structure with strong Cu—O covalent bonds inside a ZnO ionic lattice. These results are very important for further understanding in the gas sensing mechanism of Cu-ZnO-based sensors.

3.3. Photoluminescence

Fig. 4 compares the photoluminescence (PL) spectra of samples 0.5% Cu-ZnO and 3.0% Cu-ZnO measured at low temperature (10 K) and at room temperature. At both temperatures the intensity of the UV near bandgap luminescence as well as the intensity of the visible luminescence related to deep centers is by a factor of 2–3 lower in the sample 3.0% Cu-ZnO as compared to the sample 0.5% Cu-ZnO. This difference could be due to the formation of additional non-radiative recombination channels in the sample 3.0% Cu-ZnO. The visible luminescence in the 0.5% Cu-ZnO sample is located around 1.85 eV, and it is supposed to be associated with a deep unidentified acceptor with the energy level situated close to the middle of the bandgap [64,65].

The near-bandgap PL at low temperature is dominated by the donor bound exciton emission (D^0X) at 3.360 eV in both samples, as well as by a weaker band supposed to be due to donor–acceptor (DA) pair recombination with longitudinal optical-phonon replica. Most probably, a very shallow donor and a deeper acceptor are involved in this DAP transition [66,67]. The coincidence of the position of the D^0X band in both samples is an indicative that the same donor is present in both samples.

The room temperature near-bandgap PL spectrum of both samples represents a broader band resulting from the superposition of the band origination from the recombination of free excitons (FX) with its LO phonon replica.

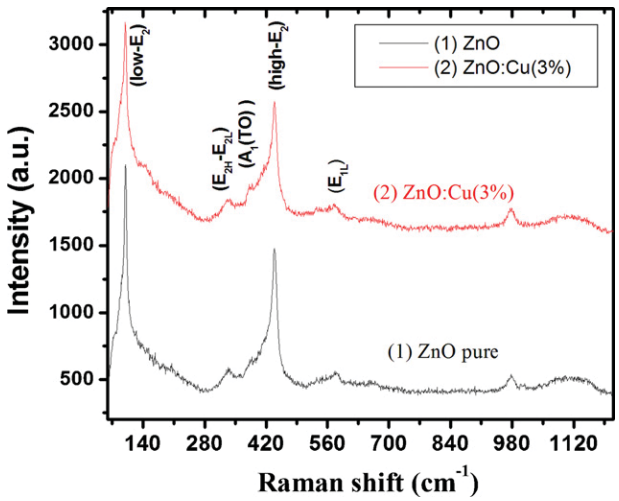

Fig. 5. Micro-Raman spectra of pure ZnO and Cu-doped ZnO on Si substrates.

Apart from these PL bands, a broad band with the maximum around 2.4–2.5 eV emerges in the low temperature spectrum of the sample with 3.0% Cu-ZnO (see Fig. 4b). This band can be associated with the Cu impurity [33,38,68]. Usually, two types of bands related to the Cu impurity are observed in this spectral range in Cu-doped ZnO samples. A structured luminescence band has been assigned to the internal transition of a hole in the Cu_{Zn} center from the excited state at $\sim E_V$ +0.4 eV to the ground state at $\sim E_C$ −0.2 eV [33,38,65 and refs. therein]. The fine structure of the emission spectrum is due to multiple phonon replicas associated with LO and local or pseudolocal vibration modes. Another structureless green luminescence band was attributed to transitions from a shallow donor to the Cu^+ state of a neutral Cu_{Zn} acceptor with a level approximately 0.5 eV above the top of the valence band [33, 69 and refs. therein]. The PL band observed in our samples is structureless. It was previously shown that the structureless band can be transformed into the structured band by annealing the samples at temperatures above 800 °C [68], and this transformation was attributed to the conversion of the Cu^+ state into the Cu^{2+} state. The temperature increase to 300 K leads to the quenching of the PL band at 2.4–2.5 eV (see Fig. 4) which is typical for the Cu-related luminescence [69]. Based on the PL analysis of broad bands in deep-level DLE emission regions one can suggest the formation of complex defects $[Cu_{Zn}—Zn_i]^x$ in Cu-ZnO [33 and refs. therein].

3.4. Micro-Raman

In order to investigate the influence of copper doping on the Raman scattering in ZnO nanostructures, room temperature micro-Raman spectra of all samples were explored. In group theory $\Gamma_{opt} = A_1(z) + 2B_1 + E_1(x,y) + 2E_2$ where x, y, z represent the polarization directions. A_1 and E_1 modes are polar and split into transverse optical (TO) and longitudinal optical (LO) components. The E_2 modes are Raman active only. The B_1 modes are infrared and Raman inactive or silent modes. It is known that the E_2(low) mode in zinc oxide is associated with the vibration of the heavy Zn sub-lattice and the E_2(high) mode involves only the oxygen atoms. The E_2(high) mode is characteristic of the wurtzite phase [31]. Fig. 5 shows a micro-Raman spectrum of Cu-doped ZnO along with the spectrum of a undoped ZnO for comparison. They are clearly indicative of good wurtzite structure of pure and doped ZnO material. No Raman peaks of CuO or Cu_2O appeared in the spectrum of the Cu-doped ZnO nanostructures, indicating

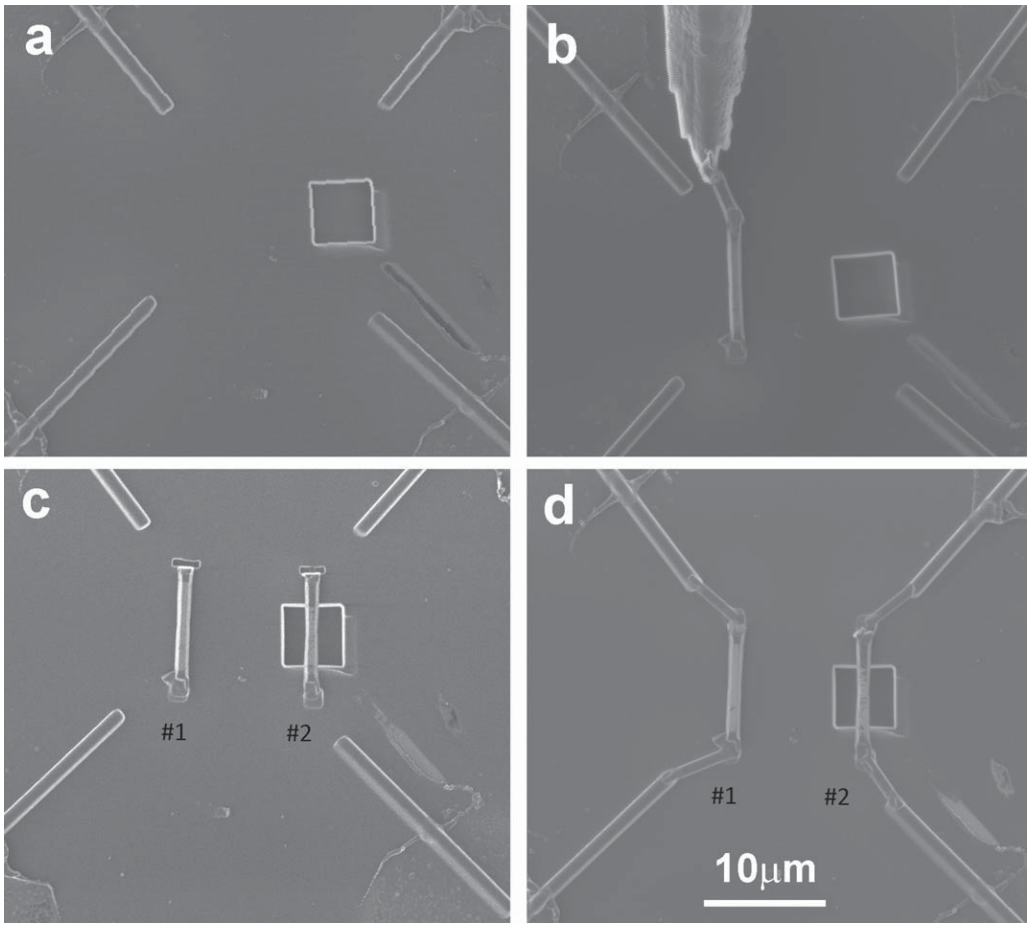

Fig. 6. SEM images showing the steps of the in situ lift-out fabrication procedure in the FIB/SEM system. (a) Four external contacts made on substrate, a square hole cut on the glass between two electrodes; (b) an intermediate ZnO rod and a single ZnO rod selected for the fabrication of the first sensor – picked – up by the FIB needle and positioned between the first two electrodes; (c) a single ZnO rod #1 and a single Cu-doped ZnO rod #2 selected for sensor fabrication placed between the contact electrodes on the same substrate; (d) single one-dimensional rod #1 (ZnO) and #2 (Cu-ZnO) welded to both electrode/external connections as final double-rod sensor.

no secondary phase in copper-doped samples, which is consistent with the XRD results. From Fig. 5 one observes the effect of Cu-doping on the E_2(high) mode of ZnO since its intensity decreases. The Raman spectrum indicates a shift in the signal at ~437 cm^{-1} for Cu-doped ZnO, which was also found in ZnO:Cu grown by other techniques [70–72]. The Raman line of the E_2(high) mode becomes broad and weaker, which means that the wurtzite crystalline structure of ZnO is weakened by high Cu doping [70] and due to formation of complex defects $[Cu_{Zn}—Zn_i]^x$ in Cu-ZnO. The frequency shift was explained by alloy potential fluctuation (APF) using the spatial correlation model by Samanta et al. [73].

The intense peak near 439 cm^{-1} due to the E_2(high) mode (Fig. 5, curve 1) displays a clear asymmetry toward low frequencies. The asymmetric line shape has been analyzed in details by Cuscó et al. [74]. It could be successfully explained in terms of resonant anharmonic interaction of the high-E_2 mode with a band of combined transverse and longitudinal acoustic modes, as the steep variation of the two-phonon density of states around the high-E_2 frequency leads to a distorted phonon line shape. We can suggest that mixing two different cations though doping in aqueous solution could affect the local polarizability by charge distribution and result in at least one vibrational mode being strongly influenced [75,76].

No differences in the Raman spectra were observed for concentration as low as 0.5% Cu as compared to pure ZnO [31].

4. Fabrication of sensors by in situ lift-out technique and Gas sensing properties

Next the in situ lift-out procedure, described in our previous works [8–10], was used to fabricate a double rod-based sensor. Details of the FIB fabrication process can be found in Refs. [8–10].

Briefly we made 4 external contacts as shown in Fig. 6a. Then, the tungsten needle with the intermediate microrod is used to place selected rods on designated places as shown in Fig. 6b and c. Fig. 6d shows the fabricated double-rod-based sensor used for comparison in the same conditions of a single ZnO rod and single 3% Cu-ZnO rod.

The fabricated double rod ZnO and Cu-ZnO-based sensor was put in a test chamber to detect H_2 and other gases, such as O_2, CH_4, CO, LPG and ethanol. It was found that resistance change $|\Delta R| = |R_{air} - R_{gas}|$ with H_2 gas introduction, where R_{air} the resistance of the sensor in air and R_{gas} is resistance in the test gas. The gas response value of the sensor was obtained using relationship: $S = |\Delta R/R_{gas}|$. After the exposure to hydrogen the sensor was maintained for a recovering period in air. The room temperature sensitivity of the single rod ZnO and single rod Cu-ZnO sensor to 200 ppm H_2 is shown in Fig. 7. Response time constants for Cu-ZnO are faster on the order of 30 ms and after 40 ms the signal reaches the equilibrium value after the H_2 test gas was injected. The relative resistance changes were about 44%. The resistance was restored within 10% above the original value within 50–90 ms of introducing clean air. This suggests a reasonable recovery time. The sensor

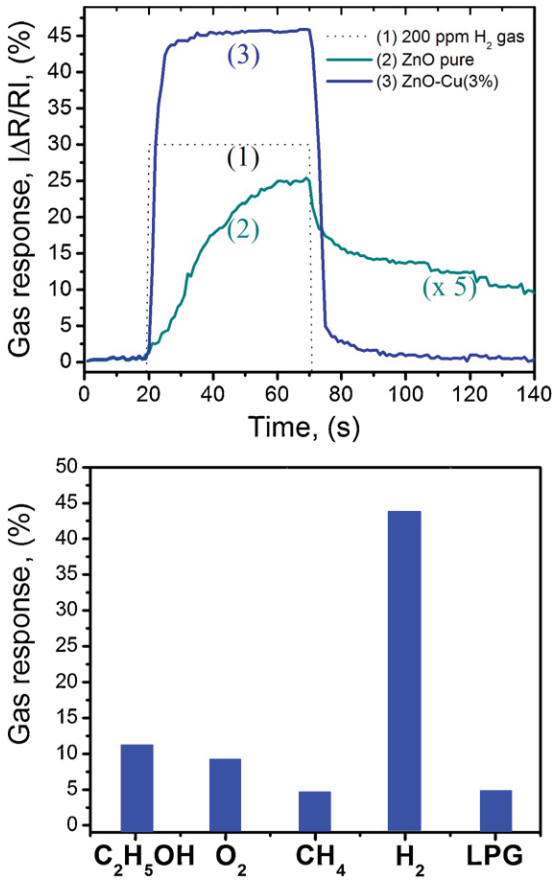

Fig. 7. (a) Room temperature relative response (multiplied by 5) of the conductometric single ZnO one-dimensional rod (curve 2) and single Cu-doped ZnO (curve 3) rod-based sensor structure fabricated by in situ lift-out technique in the FIB system to 200 ppm H_2 gas (curve 1). (b) Gas response of a Cu-ZnO rod based sensor to different ambient of 200 ppm concentration.

showed relatively fast response and baseline recovery for 200 ppm H_2 detection at room temperature. For comparison the pure ZnO rod-based sensor gas response is shown on the same figure. We can see that sensitivity is about 10 times lower with much slower time response.

For comparison sensors containing a lower Cu-doping have been submitted to 200 ppm of H_2. Improvements of about 25% and 35% in sensor response were observed for 0.5% Cu and 1% Cu doping, respectively. A significant improvement, in comparison with pure ZnO-rod based sensors, was obtained for rods doped in the range 2–3% Cu in ZnO and almost similar results were obtained, about 40% and 44%. The resistance was restored toward 10% above the original value within 25 s and 19 s of introducing clean air for 0.5% Cu and 1% Cu doping ZnO sensor, respectively.

In order to test the selectivity to H_2 of our Cu-ZnO sensor, the response to C_2H_5OH, O_2, CH_4 and LPG (Liquefied Petroleum Gas) has been investigated and summarized in Fig. 7b. We can see that the Cu-ZnO sensor's response to 200 ppm LPG and 200 ppm CH_4 is lower in comparison with its gas response to hydrogen. These data show the high selectivity of the fabricated sensor structure and the high prospect of Cu-doped ZnO as material for miniaturized sensors operating at room temperature.

Next, we would like to discuss the proposed sensing mechanism of a Cu-ZnO rod in comparison with a pure ZnO. According to the results presented in Fig. 7a, one can conclude that the Cu-ZnO sensor has a higher and faster gas response and faster recovery times than the pure ZnO sensor. The factors influencing gas sensing properties of the zinc oxide based materials and their fundamental mechanisms are still under debate. The gas sensing can be explained by the fact that hydrogen adsorbs on zinc oxide surfaces when gas is introduced in the test chamber as described before [8–10] and changes the conductance value (see Fig. 7). The adsorbed H atoms on ZnO surfaces, as for example Zn—H(a) and O—H(a), would desorb molecularly as H_2 at temperatures, of 330 K and 450 K [77]. Chan and Griffin [78] reported that the adsorbed H(a) desorbed from Zn sites at ~319 K, which proves to be in good agreement with the results reported by Kim et al. [77]. These data support our experimental observations on faster recovery times for Cu-ZnO sensors, as well as the proposed sensing mechanism. Since in our measurements we used a pico-ammeter as the power source and a nano-V meter to monitor the voltage drop on the rod-based sensor, then the rod could act as heating element and as sensing element. In such case it appears that the self-generated heat contributes the desorption of absorbed ambient molecules and gas species. The local temperature of ~150 °C on the surface of the sensing material was evaluated according to the ref. [79].

Thus, Cu-doping of zinc oxide is an approach to control the conductance value [80] and depletion width [39,40,21] of the ZnO structure, respectively to control the current flow in individual rods. For Cu-doped ZnO it is necessarily to mention that stability of the Coulomb forces of the interactions between the acceptor defect (Cu_{Zn}^{+}) and intrinsic ZnO donors (Zn_i or V_O) may occur by capture of an electron from the lattice. West et al. [33] proposed a model of an associate donor–acceptor for Cu_{Zn}, where

$$[Cu_{Zn}^{+}(3d^{10})]^{-} + Zn_I^{+}(4s^1) \rightarrow \{[Cu_{Zn}^{+}(3d^{10})]Zn_I^{+}(4s^1)\}^{0}$$

or in Kroger and Vink notations [81],

$$Cu_{Zn}^{*} + Zn_i^{*} \rightarrow [Cu_{Zn}{-}Zn_i]^{x}$$

Incorporation of Cu into ZnO reduces its conductivity as Cu introduces deep acceptor level, confirmed by our PL studies, and it traps electrons from the conduction band [39,40,21]. According to the model, the created complex defects $[Cu_{Zn}{-}Zn_i]^x$ in Cu-ZnO may contribute to the increased barrier height. The charge depletion increases due to defect states, with changing surface barrier height for electrons in the E_C. The surface depletion layers of ZnO and of Cu:ZnO with the same diameter d, but with different concentrations of charge carriers and defects are different, larger and smaller, respectively. Thus, the current flow through the conduction channel in a Cu:ZnO nanorod can be controlled better. In cases where the width of the conduction channel is thinner (closer to the critical value D_c), it depends more on the adsorbed gas species on the surface, which means that a better control of the charge carrier flow and of the gas response can be achieved. The number of adsorbed oxygen species on the rod surface would depend on the Cu doping in ZnO to adsorb the oxygen which in turn would oxidize the exposed gas. For doping in the range 2–3%Cu in zinc oxide it provides most efficient properties to promote effectively sensing due to more adsorbed oxygen on surface. For lower concentration of doping the surface may be poor in oxygen and gas response is lower, which is in agreement with previous reports [82,83]. Several other papers reported the gas selectivity and sensitivity of ZnO sensors by using Cu doping or functionalization as described in refs. [28,84–86]. When gas molecules are adsorbed on the surface, they are preferably adsorbed on the Cu sites to form bonds between them. The weak Cu—H bonding consists of the donation of H_2 electrons to the metal and the back donation of electrons from d-orbitals of Cu to H_2, and the adsorption results in the enhancement of the gas reactivity [87]. The gas adsorption mainly took place at the Cu sites and not at the Zn sites, and then H_2 molecules migrate from the Cu to the Zn sites [87]. In this way, the Cu sites enhanced the gas adsorption and thus the reaction of H_2 with oxygen species. Patil et al. [88] reported that the adsorption chemistry

of Cu-O-modified tin titanate (TT) surface would be different from the pure TT thick film surface. The CuO misfits on the surface would adsorb more oxygen species than the pure TT surface. In addition, Cu-doping can greatly improve the formation of surface oxygen vacancies in the metal oxide, and the formation energy is related to the Cu depth from the surface. Molecular O_2 can be exothermically adsorbed on the reduced SnO_2 surface, which also underlies the mechanism of enhanced sensitivity due to Cu-doping [89].

Thus, one can conclude that the gas response is affected by: depletion region sizes; concentrations of charge carriers; defect states (e.g. oxygen vacancies V_O), which favors more oxygen to be adsorbed on the surface, respectively higher gas response.

Another approach to improve the gas response is to use thinner nanowires [90], which is in our attention.

5. Conclusions

In summary, a single Cu-ZnO rod-based hydrogen sensor synthesized through a low-temperature aqueous solution route and FIB has been demonstrated for the first time. The major advantages of this method are its simplicity and fast growth rates (20 min versus several hours). We also showed that the structural and chemical properties of the rods can be effectively controlled by using suitable preparation conditions through Cu doping. Based on XRD studies, we determined that the slight difference of the lattice parameters in Cu-doped ZnO depositions is probably caused by the copper atoms occupying different positions in the ZnO lattice and the formation of complex defects $[Cu_{Zn}—Zn_i]^x$ in Cu-ZnO. We have observed a significant increase in the ratio of the oxygen XPS feature attributed to defective ZnO in the Cu-doped sample (ZnO_x/ZnO = 3.3) as compared to the undoped ZnO (ZnO_x/ZnO = 0.5) reemphasizing the incorporation of Cu^+ ions into the ZnO and the consequent generation of defects. XPS suggests on the possibility of monovalent copper in $Cu_{Zn}—V_O$ complexes (V_O represents oxygen vacancies). The photoluminescence band associated with the Cu impurity was observed as a broad band with the maximum around 2.4–2.5 eV, and it emerges in the low temperature spectrum of the sample with 3.0% Cu-ZnO. Our Raman studies indicate the good wurtzite structure of pure and doped ZnO. No Raman peaks of CuO or Cu_2O appeared in the spectrum of the Cu-doped ZnO nanostructures, indicating no secondary phase in the copper-doped samples, which is consistent with the XRD results. We observed that the Raman line of the E_2(high) mode becomes broad and weaker, which means that the wurtzite crystalline structure of ZnO is weakened by the higher Cu doping.

In addition we presented for the first time a double rod-based sensor made by a bottom-up approach by using in situ lift-out technique. Furthermore, an enhancement of 44% in sensitivity to H_2 followed by fast response and recovery time (compared to pure ZnO), as well as a better selectivity were found to be useful for further development of H_2 sensor at room temperature. For comparison sensor response of 25% and 35% were measured for 0.5% Cu and 1% Cu doped ZnO nanorods, respectively. For doping in the range 2–3% Cu in ZnO we obtained almost similar results, about 40% and 44%. The resistance was restored toward the 10% above the original value within 25 s and 19 s of introducing clean air for 0.5% Cu and 1% Cu doping-ZnO sensor, respectively.

Acknowledgments

BRC acknowledges the financial support from the National Science Foundation (NSF-DMR-0906562). Dr. Lupan acknowledges UCF for support as an invited researcher at the Physics Department.

References

[1] O'M. Bockris, Hydrogen economy in the future, International Journal of Hydrogen Energy 24 (1999) 1–15.
[2] L. Barreto, A. Makihira, K. Riahi, The hydrogen economy in the 21st century: a sustainable development scenario, International Journal of Hydrogen Energy 28 (2003) 267–284.
[3] T. Hübert, L. Boon-Brett, G. Black, U. Banach, Hydrogen sensors – a review, Sensors and Actuators B 157 (2011) 329–352.
[4] V.M. Aroutiounian, Metal oxide hydrogen, oxygen, and carbon monoxide sensors for hydrogen setups and cells: review, International Journal of Hydrogen Energy 32 (2007) 1145–1158.
[5] V.M. Aroutiounian, Hydrogen detectors, International Scientific Journal for Alternative Energy and Ecology 3 (23) (2005) 21–31.
[6] F. Rumiche, H.H. Wang, J.E. Indacochea, Development of a fast-response/high-sensitivity double wall carbon nanotube nanostructured hydrogen sensor, Sensors and Actuators B 163 (2012) 97–106.
[7] G. Shen, fabrication and characterization of metal oxide nanowire sensors, Recent Patents on Nanotechnology 2 (2008) 160–168.
[8] O. Lupan, G. Chai, L. Chow, Fabrication of ZnO nanorod-based hydrogen gas nanosensor, Microelectronics Journal 38 (2007) 1211–1216.
[9] O. Lupan, G. Chai, L. Chow, Novel hydrogen gas sensor based on single ZnO nanorod, Microelectronic Engineering 85 (2008) 2220–2226.
[10] O. Lupan, V.V. Ursaki, G. Chai, L. Chow, G.A. Emelchenko, I.M. Tiginyanu, A.N. Gruzintsev, A.N. Redkin, Selective hydrogen gas nanosensor using individual ZnO nanowire with fast response at room temperature, Sensors and Actuators B 144 (2010) 56–66.
[11] S.N. Das, J.P. Kar, J.H. Choi, T.I. Lee, K.J. Moon, J.M. Myoung, Fabrication and characterization of ZnO single nanowire-based hydrogen sensor, Journal of Physical Chemistry C 114 (2010) 1689–1693.
[12] I.M. Tiginyanu, O. Lupan, V.V. Ursaki, L. Chow, M. Enachi, Nanostructures of metal oxides, Comprehensive Semiconductor Science & Technology 105 (2011) 396–479.
[13] B.S. Kang, Y.W. Heo, L.C. Tien, D.P. Norton, F. Ren, B.P. Gila, S.J. Pearton, Hydrogen and ozone gas sensing using multiple ZnO nanorods, Applied Physics A 80 (2005) 1029–1032.
[14] G.Y. Chai, O. Lupan, E.V. Rusu, G.I. Stratan, V.V. Ursaki, V. Şontea, H. Khallaf, L. Chow, Functionalized individual ZnO microwire for natural gas detection, Sensors and Actuators A: Physical 176 (2012) 64–71.
[15] P. Patnaik, A Comprehensive Guide to the Hazardous Properties of Chemical Substances, Wiley-Interscience, 2007, ISBN 0-471-71458-5, p. 402.
[16] D.J. Norris, A.L. Efros, S.C. Erwin, Doped nanocrystals, Science 319 (2008) 1776–1779.
[17] J.J. Shim, T. Hwang, S. Lee, J.H. Park, S.-J. Han, et al., Origin of ferromagnetism in Fe and Cu-codoped ZnO, Applied Physics Letters 86 (2005) 082503.
[18] D.B. Buchholz, R.P.H. Chang, J.H. Song, J.B. Ketterson, Room temperature ferromagnetism in Cu-doped ZnO thin films, Applied Physics Letters 87 (2005) 082504.
[19] D. Chakraborti, J. Narayan, J.T. Prater, Room temperature ferromagnetism in $Zn_{1-x}Cu_xO$ thin films, Applied Physics Letters 90 (2007) 062504.
[20] C. Sudakar, J.S. Thakur, G. Lawes, R. Naik, V.M. Naik, Ferromagnetism induced by planar nanoscale CuO inclusion in Cu-doped ZnO thin films, Physical Review B 75 (2007) 054423.
[21] T.S. Herng, S.P. Lau, S.F. Yu, S.H. Tsang, K.S. Teng, J.S. Chen, Ferromagnetic Cu doped ZnO as an electron injector in heterojunction light emitting diodes, Journal of Applied Physics 104 (2008) 103104.
[22] D. Gao, Y. Xu, Z. Zhang, H. Gao, D. Xue, Room temperature ferromagnetism of Cu doped ZnO nanowires arrays, Journal of Applied Physics 105 (2009) 063903.
[23] C. Xu, K. Yang, L. Huang, H. Wang, Cu-doping induced ferromagnetism in ZnO nanowires, Journal of Chemical Physics 130 (2009) 124711.
[24] Y. Tian, Y. Li, M. He, I.A. Putra, H. Peng, et al., Bound magnetic polarons and p-d interaction in ferromagnetic insulating Cu-doped ZnO, Applied Physics Letters 98 (2011) 162503.
[25] Y.S. Sonawane, K.G. Kanade, B.B. Kale, R.C. Aiyer, Electrical and gas sensing properties of self-aligned copper-doped zinc oxide nanoparticles, Materials Research Bulletin 43 (2008) 2719–2726.
[26] F.D. Paraguay, M. Miki-Yoshida, J. Morales, J. Solis, W.L. Estrada, Influence of Al, In, Cu, Fe, and Sn dopants on the response of thin film ZnO gas sensor to ethanol vapor, Thin Solid Films 373 (2000) 137–140.
[27] H. Gong, J.Q. Hu, J.H. Wang, C.H. Ong, F.R. Zhu, Nano-crystalline Cu-doped ZnO thin film gas sensor for CO, Sensors and Actuators B 115 (2006) 247–251.
[28] M. Zhao, X. Wang, L. Ning, J. Jia, X. Li, L. Cao, Electrospun Cu-doped ZnO nanofibers for H_2S sensing, Sensors and Actuators B 156 (2011) 588–592.
[29] A. Ghosh, A. Ghule, R. Sharma, Effect of Cu doping on LPG sensing properties of soft chemically grown nano-structured ZnO thin film, Journal of Physics: Conference Series 365 (2012) 012022.
[30] J. Liu, L. Xu, B. Wei, W. Lv, H. Gao, X. Zhang, One-step hydrothermal synthesis and optical properties of aluminum doped ZnO hexagonal nanoplates on a zinc substrate, CrystEngComm 13 (2011) 1283–1286.
[31] O. Lupan, L. Chow, L.K. Ono, B. Roldan Cuenya, G. Chai, H. Khallaf, S. Park, A. Schulte, Synthesis and characterization of Ag- or Sb-doped ZnO nanorods by a facile hydrothermal route, The Journal of Physical Chemistry C 114 (2010) 12401–12408.
[32] M.B. Rahmani, S.H. Keshmiri, M. Shafiei, K. Latham, W. Wlodarski, J. du Plessis, K. Kalantar-Zadeh, Transition from n- to p-type of spray pyrolysis deposited Cu doped ZnO thin films for NO_2 sensing, Sensor Letters 7 (2009) 621–628.

[33] C. West, D.J. Robbins, P.J. Dean, W. Hays, The luminescence of copper in zinc oxide, Physica B & C 116 (1983) 492–499.
[34] M. Oztas, M. Bedir, Thickness dependence of structural, electrical and optical properties of sprayed ZnO:Cu films, Thin Solid Films 516/8 (2008) 1703–1709.
[35] J.B. Kim, D. Byun, S.Y. Ie, D.H. Park, W.K. Choi, C. Ji-Won, A. Basavaraj, Cu-doped ZnO-based p–n hetero-junction light emitting diode, Semiconductor Science and Technology 9 (2008) 095004.
[36] K.S. Ahn, T. Deutsch, Y. Yan, C.S. Jiang, C.L. Perkins, J. Turner, M. Al-Jassim, Synthesis of band-gap-reduced p-type ZnO films by Cu incorporation, Journal of Applied Physics 102 (2007), 023517-023517-6.
[37] H.Y. Bae, G.M. Choi, Electrical and reducing gas sensing properties of ZnO and ZnO–CuO thin films fabricated by spin coating method, Sensors and Actuators B: Chemical 55 (1999) 47–54.
[38] R. Dingle, Luminescent transitions associated with divalent copper impurities and the green emission from semiconducting zinc oxide, Physical Review Letters 23 (1969) 579–581.
[39] T.S. Herng, S.P. Lau, S.F. Yu, H.Y. Yang, K.S. Teng, J.S. Chen, Ferromagnetic copper-doped ZnO deposited on plastic substrates. Journal of Physics: Condensed Matter 19 (2007) 236214.
[40] S.J. Pearton, D.P. Norton, K. Ip, Y.W. Heo, T. Steiner, Recent advances in processing of ZnO, Journal of Vacuum Science and Technology B 22 (2004) 932–948.
[41] G. Xing, G. Xing, M. Li, E.J. Sie, D. Wang, A. Sulistio, Q. Ye, C. Hon Alfred Huan, T. Wu, T.C. Sum, Charge transfer dynamics in Cu-doped ZnO nanowires, Applied Physics Letters 98 (2011) 102105.
[42] O. Lupan, L. Chow, G. Chai, B. Roldan Cuenya, A. Naitabdi, A. Schulte, H. Heinrich, Nanofabrication and characterization of ZnO nanorod arrays and branched microrods by aqueous solution route and rapid thermal processing, Materials Science and Engineering B 145 (2007) 57–66.
[43] O. Lupan, T. Pauporte, B. Viana, Low-temperature growth of ZnO nanowire arrays on p-silicon (1 1 1) for visible-light-emitting diode fabrication, Journal of Physical Chemistry C 114 (2010) 14781–14785.
[44] American Society for Testing and Material, Powder Diffraction Files, Joint Committee on Powder Diffraction Standards, Swarthmore, PA, 1999, pp. 3–888.
[45] T.S. Herng, S.P. Lau, S.F. Yu, H.Y. Yang, L. Wang, M. Tanemura, J.S. Chen, Magnetic anisotropy in the ferromagnetic Cu-doped ZnO nanoneedles, Applied Physics Letters 90 (2007) 032509.
[46] Z. Zhang, J.B. Yi, J. Ding, L.M. Wong, H.L. Seng, S.J. Wang, J.G. Tao, G.P. Li, G.Z. Xing, T.C. Sum, C.H. Alfred Huan, T. Wu, Cu-doped ZnO nanoneedles and nanonails: morphological evolution and physical properties, Journal of Physical Chemistry C 112 (2008) 9579–9585.
[47] O. Lupan, Th. Pauporté, T. Le Bahers, B. Viana, I. Ciofini, Wavelength emission tuning of ZnO nanowires-based light emitting diodes by Cu-doping: experimental and computational insights, Advanced Functional Materials 21 (2011) 3564–3572.
[48] R.D. Shannon, Revised effective ionic radii and systematic studies of interatomic distances in halides and chalcogenides, Acta Crystallographica. Section A, Crystal Physics, Diffraction, Theoretical and General Crystallography 32 (1976) 751–767.
[49] Q. Ma, D.B. Buchholz, R.P.H. Chang, Local structures of copper-doped ZnO films, Physical Review B 78 (2008) 214429.
[50] Y. Yan, M.M. Al-Jassim, S.H. Wei, Doping of ZnO by group-IB elements, Applied Physics Letters 89 (2006) 181912.
[51] O. Lupan, T. Pauporté, L. Chow, B. Viana, F. Pellé, B. Roldan Cuenya, L.K. Ono, H. Heinrich, Effects of annealing on properties of ZnO thin films prepared by electrochemical deposition in chloride medium, Applied Surface Science 256 (2010) 1895–1907.
[52] O. Lupan, T. Pauporté, B. Viana, P. Aschehoug, Electrodeposition of Cu-doped ZnO nanowire arrays and heterojunction formation with p-GaN for color tunable light emitting diode applications, Electrochimica Acta 56 (2011) 10543–10549.
[53] T. Matsuhisa, in Catalysis, a Specialist Periodical report, Vol. 12, J.J. Spivey, The royal Society of Chemistry, Cambridge, UK, (1996), Chapter I.
[54] D.L. Hou, X.J. Ye, H.J. Meng, H.J. Zhou, X.L. Li, C.M. Zhen, G.D. Tang, Magnetic properties of n-type Cu-doped ZnO thin films, Applied Physics Letters 90 (2007) 142502.
[55] M. Shuai, L. Liao, H.B. Lu, L. Zhang, J.C. Li, D. Fu, Room-temperature ferromagnetism in Cu^+ implanted ZnO nanowires, Journal of Physics D: Applied Physics 41 (2008) 135010.
[56] B.E. Goodby, J.E. Pemberton, XPS characterization of a commercial $Cu/ZnO/Al_2O_3$ catalyst: effects of oxidation, reduction, and the steam reformation of methanol, Applied Spectroscopy 42 (1988) 754–760.
[57] P. Lazcano, M. Batzill, U. Diebold, P. Haberle, Oxygen adsorption on Cu/ZnO(0 0 0 1)–Zn, Physical Review B 77 (2008) 035435.
[58] W.M.K.P. Wijekoon, M.Y.M. Lyktey, P.N. Prasad, J.F. Garvey, The nature of copper in thin films of copper iodide grown by laser-assisted molecular beam deposition: comparative ESCA and EDXS studies, Journal of Physics D: Applied Physics 27 (1994) 1548–1555.
[59] D. Chakraborti, J. Narayan, J.T. Prater, Room temperature ferromagnetism in $Zn_{1-x}Cu_xO$ thin films, Applied Physics Letters 90 (2007) 062504.
[60] H.J. Xu, H.C. Zhu, X.D. Shan, Y.X. Liu, J.Y. Gao, X.Z. Zhang, J.M. Zhang, P.W. Wang, Y.M. Hou, D.P. Yu, Effects of annealing on the ferromagnetism and photoluminescence of Cu-doped ZnO nanowires, Journal of Physics: Condensed Matter 22 (2010) 016002.
[61] K. Ozawa, T. Sato, Y. Oba, K. Edamoto, Electronic structure of Cu on ZnO(1 0 −1 0): angle-resolved photoemission spectroscopy study, Journal of Physical Chemistry C 111 (2007) 4256–4263.
[62] K. Klier, Methanol synthesis, Advances in Catalysis 31 (1982) 243–313.
[63] W.P.A. Jansen, J. Beckers, J.C. Van der Heuvel, A.W.D. Van der Gon, A. Bliek, H.H. Brongersma, Dynamic behavior of the surface structure of $Cu/ZnO/SiO_2$ catalysis, Journal of Catalysis 210 (2002) 229–236.
[64] Ü. Özgür, I. Alivov Ya, C. Liu, A. Teke, M.A. Reshchikov, S. Doğan, V. Avrutin, S.-J. Cho, H. Morkoç, A comprehensive review of ZnO materials and devices, Journal of Applied Physics 98 (2005) 041301.
[65] L.M. Kukreja, P. Misra, J. Fallert, D.M. Phase, H. Kalt, Correlation of spectral features of photoluminescence with residual native defects of ZnO thin films annealed at different temperatures, Journal of Applied Physics 112 (2012) 013525.
[66] K. Nakahara, H. Takasu, P. Fons, A. Yamada, K. Iwata, K. Matsubara, R. Hunger, S. Niki, Interactions between gallium and nitrogen dopants in ZnO films grown by radical-source molecular-beam epitaxy, Applied Physics Letters 79 (2001) 4139–4141.
[67] V.V. Ursaki, I.M. Tiginyanu, V.V. Zalamai, V.M. Masalov, E.N. Samarov, G.A. Emelchenko, F. Briones, Photoluminescence of ZnO layers grown on opals by chemical deposition from zinc nitrate solution, Semiconductor Science and Technology 19 (2004) 851–854.
[68] N.Y. Garces, L. Wang, L. Bai, N.C. Giles, E. Halliburton, G. Cantwell, Role of copper in the green luminescence from ZnO crystals, Applied Physics Letters 81 (2002) 622–624.
[69] M.A. Reshchikov, V. Avrutin, N. Izyumskaya, R. Shimada, H. Morkoç, S.W. Novak, About the Cu-related green luminescence band in ZnO, Journal of Vacuum Science and Technology B 27 (2009) 1749–1754.
[70] P.K. Sharma, R.K. Dutta, A.C. Pandey, Doping dependent room-temperature ferromagnetism and structural properties of dilute magnetic semiconductor $ZnO:Cu^{2+}$ nanorods, Journal of Magnetism and Magnetic Materials 321 (2009) 4001–4005.
[71] T.L. Phan, R. Vincent, D. Cherns, N.X. Nghia, V.V. Ursaki, Raman scattering in Me-doped ZnO nanorods (Me = Mn, Co, Cu and Ni) prepared by thermal diffusion, Nanotechnology 19 (2008) 475702.
[72] Z. Wang, H. Zhang, L. Zhang, J. Yang, S. Yan, C. Wang, Low-temperature synthesis of ZnO nanoparticles by solid-state pyrolytic reaction, Nanotechnology 14 (2003) 11–15.
[73] K. Samanta, P. Bhattacharya, R.S. Katiyar, W. Iwamoto, P.G. Pagliuso, C. Rettori, Raman scattering studies in dilute magnetic semiconductor $Zn_{1-x}Co_xO$, Physical Review B 73 (2006) 245213.
[74] R. Cuscó, E. Alarcón-Lladó, J. Ibáñez, L. Artús, J. Jiménez, B. Wang, M. Callahan, Temperature dependence of Raman scattering in ZnO, Physical Review B 75 (2007) 165202.
[75] X.F. Wang, J.B. Xu, X.J. Yu, K. Xue, X. Zhao, Structural evidence of secondary phase segregation from the Raman vibrational modes in $Zn_{1-x}Co_xO$ ($0 < x < 0.6$), Applied Physics Letters 91 (2007) 031908.
[76] C.F. Windisch, G.J. Exarhos, R.R. Owings, Vibrational spectroscopic study of the site occupancy distribution of cations in nickel cobalt oxides, Journal of Applied Physics 95 (2004) 5435.
[77] W. Kim, G. Kwak, M. Jung, S.K. Jo, J.B. Miller, A.J. Gellman, K. Yong, Surface and internal reactions of ZnO nanowires: etching and bulk defect passivation by H atoms, Journal of Physical Chemistry C (2012), http://dx.doi.org/10.1021/jp304191m, Article ASAP.
[78] L. Chan, G.L. Griffin, Temperature programmed desorption studies of hydrogen on Zn(0 0 0 1) surfaces, Surface Science 145 (1984) 185–196.
[79] J.D. Prades, R. Jimenez-Diaz, F. Hernandez-Ramirez, A. Cirera, A. Romano-Rodriguez, J.R. Morante, An experimental method to estimate the temperature of individual nanowires, International Journal of Nanotechnology (2009) 783675.
[80] K. Zhen Zhou, T. Kato, M. Komaki, H. Yoshino, M. Yukawa, K. Morinaga, K. Morita, Electrical conductivity of Cu-doped ZnO and its change with hydrogen implantation, Journal of Electroceramics 11 (2003) 73–79.
[81] F.A. Kröger, H.J. Vink, Relations between the concentrations of imperfections in crystalline solids, Solid State Physics 3 (1956) 307–435.
[82] M.S. Wagh, G.H. Jain, D.R. Patil, S.A. Patil, L.A. Patil, Sensors and Actuators B 115 (2006) 128–133.
[83] A.V. Patil, C.G. Dighavkar, S.K. Sonawane, S.J. Patil, R.Y. Borse, Formulation, Characterization of Cu doped ZnO thick films as LPG gas sensor, Sensors & Transducers Journal 9 (2010) 11–20.
[84] S. Aygun, D. Cann, Hydrogen sensitivity of doped CuO/ZnO heterocontact sensors, Sensors and Actuators B 106 (2005) 837–842.
[85] W.J. Moon, J.H. Yu, G.M. Choi, The CO and H_2 gas selectivity of CuO-doped SnO_2–ZnO composite sensor, Sensors and Actuators B: Chemical 87 (2002) 464.
[86] A. Galdikas, A. Mironas, A. Šetkus, Copper-doping level effect on sensitivity and selectivity of tin oxide thin-film gas sensor, Sensors and Actuators B: Chemical 26 (1995) 29–32.
[87] H.Y. Chen, S.P. Lau, L. Chen, J. Lin, C.H.A. Huan, K.L. Tan, J.S. Pan, Synergism between Cu and Zn sites in Cu/Zn catalysts for methanol synthesis, Applied Surface Science 152 (3-4) (1999) 193–199.
[88] S.A. Patil, L.A. Patil, D.R. Patil, G.H. Jain, M.S. Wagh, CuO-modified tin titanate thick film resistors as H_2-gas sensors, Sensors and Actuators B: Chemical 123 (2007) 233–239.

[89] W. Wei, Y. Dai, B. Huang, Role of Cu doping in SnO_2 sensing properties toward H_2S, Journal of Physical Chemistry C 115 (2011) 18597–18602.
[90] S. Xu, Z.L. Wang, One-dimensional ZnO nanostructures: solution growth and functional properties, Nano Research 4 (11) (2011) 1013–1098.

Biographies

Lee Chow is a professor at the Department of Physics University of Central Florida, Orlando. He received his B.S. in physics in 1972 from the National Central University, Taiwan. He received Ph.D. in physics from Clark University, Worcester, MA, USA in 1981. In 1980–1982 he was a postdoc in physics at the University of North Carolina, Chapel Hill, NC. He joined University of Central Florida in 1983 as an assistant professor, and was promoted to associate professor in 1988 and to professor in 1998. Areas of expertise: Chemical bath deposition, nanofabrications of carbon nanotubes and metal oxides, diffusion in semiconductors, high T_c and diamond thin films.

Oleg Lupan received his M.S. in microelectronics and semiconductor devices from the Technical University of Moldova (TUM) in 1993. He received his Ph.D. in solid state electronics, microelectronics and nanoelectronics from the Institute of Applied Physics, Academy of Sciences of Moldova (ASM) in 2005. His post-doctorate research activities were carried out at the French CNRS, Paris, France and University of Central Florida, USA. He received his doctor habilitate degree in 2011 from the Institute of Electronic Engineering and Nanotechnologies of ASM. He is an associate professor and researcher scientist in solid state electronics, microelectronics and nanoelectronics at the Department of Microelectronics and Semiconductor Devices of the TUM. His current research interests range over sensors, optoelectronic devices and nanodevices.

Guangyu Chai is the research director at Apollo Technologies, Inc., Orlando, FL, USA. He received his B.S. in physics in 1999 from the Peking University, Beijing, China. He received Ph.D. in condensed matter physics from University of Central Florida, Orlando, FL, USA in 2004. Research interest: ZnO nanorod sensors; individual carbon nanotube devices; focused ion beam fabrication of nanodevices.

Hani M.M. Khallaf is a lecturer at College of Sciences, El-Minia University. He received his B.S. in physics in 1998 from the Department of Physics, El-Minia University, Egypt. He received M.Sc. in 2005 and Ph.D. in 2009 in condensed matter physics from University of Central Florida, Orlando, FL, USA. In 2010 he joined the Nanophotonic Device Research Group at CREOL; The College of Optics & Photonics, University of Central Florida as a post-doctoral research associate. Research interests: liquid phase deposition/chemical bath deposition of group II–VI semiconductor thin film materials for solar cells applications; organic photovoltaics.

Luis Katsuya Ono is currently a post-doctoral scholar at the Interdisciplinary Nanoscience Center at Aarhus University in Denmark. He obtained a B.S. in physics/microelectronics in 2000 at the University of Sao Paulo (Brazil), a M.S in nuclear engineering at Kyoto University (Japan), and Ph.D. in physics in 2009 at the University of Central Florida (USA) for his investigations of the catalytic properties of metal nanoparticles.

Beatriz Roldan Cuenya is a professor in the Department of Physics at the University of Central Florida (UCF). She joined UCF in 2004 after her postdoctoral research in the Department of Chemical Engineering at the University of California Santa Barbara (2001–2003). She obtained her Ph.D. from the Department of Physics at the University of Duisburg-Essen (Germany) summa cum laude in 2001. She completed her M.S./B.S. in physics with a minor in materials science from the University of Oviedo, Spain in 1998. Her research program explores novel physical and chemical properties of size- and shape-selected nanostructures, with emphasis on advancements in nanocatalysis. www.physics.ucf.edu/~roldan.

Ion Tiginyanu received his Ph.D. degree in semiconductor physics from Lebedev Institute of Physics, Moscow, in 1982. From 1984 to 1998 he worked as senior researcher at the Academy of Sciences of Moldova (ASM). In 2004 he was elected vice-president of the ASM. He serves as director of the National Center for Materials Study and Testing. His research interests are related to nanotechnologies, photonic crystals, random lasing, cost-effective solar cells and new sensor technologies. He has 250 journal publications and 42 patents. He is member of AAAS, OSA, SPIE, MRS and Electrochemical Society. More information is available at http://www.ncmst.utm.md.

Veaceslav V. Ursaki received his M.S. degree from the Moscow Institute of Physics and Engineering in 1979. He received his Ph.D. degree in semiconductor physics from Lebedev Institute of Physics, Academy of Sciences of U.S.S.R., in 1986, and his Doctor habilitate degree in 1998 from the Institute of Applied Physics of the Academy of Sciences of Moldova. From 1986 he works at the Institute of Applied Physics of the Academy of Sciences of Moldova. His research interests are in the field of optical properties of semiconductor materials, lasing effects in solid state nanostructures, optoelectronic and photonic properties of nanostructures and nanocomposite materials.

Victor Sontea received his M.S. degree in microelectronics and semiconductor devices from the Polytechnic Institute of Chişinău, Moldova in 1973. He received his Ph.D. degree in semiconductor physics from the Institute of Applied Physics of the Academy of Sciences of Moldova of U.S.S.R., in 1982. He was promoted to professor in 1996. Since 1973 he works at the Technical University of Moldova (TUM). His research interests are in the Microelectronics, physics and technology of materials, semiconductor devices and micro-nano-electronics, engineering of micro-nano-electronics and biomedical devices.

Alfons Schulte is a professor in the Department of Physics and a joint faculty in the College of Optics and Photonics at the University of Central Florida. He joined UCF in 1990 following postdoctoral research at the University of Illinois at Urbana-Champaign (UIUC) and the IBM Almaden research laboratory. He obtained his doctorate in Physics from the Technical University Munich summa cum laude in 1985. He held appointments as a visiting scholar at UIUC and Los Alamos National Laboratory (1997/1998) and as professor at the TU Munich (2001/2002). His research interests include biological physics, optical spectroscopy at the single cell level, and applications of light-scattering spectroscopies to optical and nano-materials.